of a complete monolayer is most favorable at low Co(II) concentrations. This observation contrasts with results reported by Hills et al.[21] for monolayer formation during the reduction of Ni(II) and Ag(I) in LiCl-KCl eutectic. These workers reported that monolayer formation was relatively independent of the substrate ion concentration. In the present case this process could hardly be described as underpotential deposition in the thermodynamic sense, because $E_X°$ for the Co(II)/Co couple is positive of the predeposition wave by about 0.5 V. In addition, most reported $E_{1/2}$ values for Co(II) reduction in inorganic chloroaluminate melts are also significantly positive of the potential reported for this predeposition wave. A complete explanation of this phenomenon awaits further, more detailed studies.

Acknowledgment. Support of this work by a Hooker Chemical Corp. Grant of the Research Corp. and by a University of Mississippi Faculty Research Grant is gratefully acknowledged.

Registry No. BPC, 1124-64-7; $AlCl_3$, 7446-70-0; $Co(Al_2Cl_7)_2$, 37308-38-6; $CoCl_4^{2-}$, 14337-08-7.

(21) Hills, G. J.; Schiffrin, D. J.; Thompson, J. *J. Electrochem. Soc.* **1973**, *120*, 157.

Contribution from the Christopher Ingold Laboratories, University College, London WC1H OAJ, England, and the Department of Chemistry, Queen Mary College, London E1, England

Crystal Structure and Electronic, Infrared, Raman, and Resonance Raman Spectra of the Mixed-Valence, Halogen-Bridged, Anion-Chain Complexes $Cs_2[Pt^{II}(NO_2)(NH_3)X_2][Pt^{IV}(NO_2)(NH_3)X_4]$, X = Br or I

ROBIN J. H. CLARK,* MOHAMEDALLY KURMOO, ANITA M. R. GALAS, and MICHAEL B. HURSTHOUSE

Received February 19, 1981

The complexes $Cs_2[Pt^{II}(NO_2)(NH_3)X_2][Pt^{IV}(NO_2)(NH_3)X_4]$, with X = Br or I, consist of infinite, almost linear, chains in which the halogen atoms link the *trans*-$Pt(NO_2)(NH_3)X_2$ units. The crystal structures of both salts were refined within the space group *Pnam* (four $CsPt(NO_2)(NH_3)X_3$ units per unit cell) to final *R* factors of 0.036 (X = Br) and 0.038 (X = I). The chains of $[Pt^{II}(NO_2)(NH_3)X_2][Pt^{IV}(NO_2)NH_3X_4]$ are longitudinally disordered so that all Pt atom sites comprise $^1/_2Pt^{II} + {}^1/_2Pt^{IV}$ and the axial X atoms half occupy two positions ~0.6-0.8 Å apart. The key bond lengths are as follows: Pt-NH_3, 2.076 (bromide) and 2.067 Å (iodide); Pt-NO_2, 2.064 (bromide) and 2.033 Å (iodide); Pt-Br_{ax}, 2.492 Å; Pt-Br_{eq}, 2.443 Å; Pt-I_{ax}, 2.711 Å; Pt-I_{eq}, 2.631 Å. The complexes are strongly colored and highly dichroic and exhibit very rich and detailed resonance Raman spectra when irradiated within the contour of the $Pt^{II} \rightarrow Pt^{IV}$ intervalence band at 19 000 (bromide) and 12 800 cm^{-1} (iodide). In particular, for the bromide, 11 three-or-more-membered progressions were observed, for nine of which ν_1, the symmetric Br-Pt^{IV}-Br stretching mode at 178 cm^{-1}, acts as the progression-forming mode. The results imply a substantial change in the Pt-X_{ax} bond length in the intervalence state for each complex together with other smaller changes in the Pt-X_{eq} and nitro group bonds in this state.

Introduction

The electronic, infrared, Raman, and resonance Raman (RR) spectra of a variety of linear-chain, halogen-bridged complexes of platinum have now been studied,[1-6] in particular those cases in which the infinite chains are either cationic (A)

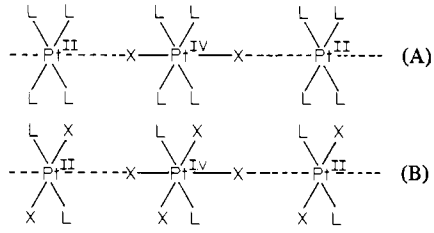

(L = neutral amine, X = Cl, Br, or I)

or neutral (B). Such complexes are deeply colored, strongly dichroic, and semiconducting along the chain axis (though insulating perpendicular thereto). The color is attributed to the axially polarized $Pt^{II} \rightarrow Pt^{IV}$ intervalence transition. Irradiation within the contour of the intervalence band leads in all cases to the appearance in the RR spectra of long progressions in which ν_1, ν(X-Pt^{IV}-X), the symmetric Pt-X stretching mode, acts as the progression-forming mode. However, few studies of anion chain complexes have yet been made and such complexes have, in general, yielded unremarkable RR spectra.[7] Two further platinum complexes, initially prepared and formulated as $Cs[Pt(NO_2)(NH_3)Br_{3.25}]$ and $Cs[Pt(NO_2)(NH_3)I_3]$ by Muraveiskaya et al.,[8,9] have recently been reformulated as class II mixed-valence complexes $Cs_2[Pt^{II}(NO_2)(NH_3)X_2][Pt^{IV}(NO_2)(NH_3)X_4]$ by Seth et al.,[10] principally on the basis of analytical, photoelectron, and electrical conductance studies. These complexes afford the opportunity for very detailed RR studies on a particular type of anion chain complex, the reformulation of which appeared to be correct on the basis of the high anisotropy of their optical absorption and electrical conductance. The present investigation is therefore concerned with (a) the determination of the crystal structure of the two nitro complexes, proving their

* To whom correspondence should be addressed at University College.

(1) Clark, R. J. H. *Ann. N.Y. Acad. Sci.* **1978**, *313*, 672 and references therein.
(2) Clark, R. J. H.; Turtle, P. C. *Inorg. Chem.* **1978**, *17*, 2526.
(3) Campbell, J. R.; Clark, R. J. H.; Turtle, P. C. *Inorg. Chem.* **1978**, *17*, 3622.
(4) Clark, R. J. H.; Kurmoo, M. *Inorg. Chem.* **1980**, *19*, 3522.
(5) Clark, R. J. H.; Kurmoo, M.; Buse, K. D.; Keller, H. J. *Z. Naturforsch. B: Anorg. Chem., Org. Chem.* **1980**, *35B*, 1272.
(6) Clark, R. J. H.; Kurmoo, M.; Keller, H. J.; Keppler, B.; Traeger, U. *J. Chem. Soc., Dalton Trans.* **1980**, 2498.
(7) Papavassiliou, G. C.; Layek, D. *Z. Naturforsch. B: Anorg. Chem., Org. Chem.* **1980**, *35B*, 676. Clark, R. J. H.; Kurmoo, M., unpublished work.
(8) Muraveiskaya, G. S.; Antokol'skaya, I. I. *Russ. J. Inorg. Chem.* **1970**, *15*, 373.
(9) Koz'min, P. A.; Surazhskaya, M. D.; Muraveiskaya, G. S.; Antokol'skaya, I. I. *Russ. J. Inorg. Chem.* **1971**, *16*, 302.
(10) Seth, P. N. A.; Underhill, A. E.; Watkins, D. M. *J. Inorg. Nucl. Chem.* **1980**, *42*, 1151.

0020-1669/81/1320-4206$01.25/0

Table I. Details of Crystal Data, Intensity Measurements, and Refinements for $Cs_2[Pt^{II}(NO_2)(NH_3)X_2][Pt^{IV}(NO_2)(NH_3)X_4]$

	X = Br	X = I
Crystal Data		
M_r	630.758	771.743
crystal system	orthorhombic	orthorhombic
a/Å	15.7685 (14)	16.7383 (11)
b/Å	10.1497 (9)	10.5430 (7)
c/Å	5.8197 (7)	6.0627 (6)
α/deg	90	90
β/deg	90	90
γ/deg	90	90
V/Å^3	931.4	1069.9
space group	*Pnam*	*Pnam*
Z	4	4
D_c/g cm^{-3}	4.498	4.791
D_m	not measured	not measured
$F(000)$	1084	1300
μ(Mo Kα)/cm^{-1}	307.2	238.6
Data Collection		
crystal dimens/mm	0.55 × 0.05 × 0.08	0.50 × 0.15 × 0.0085
θ min, θ max/deg	1.5, 25.0	1.5, 30.0
scan width parameters A, B	0.85, 0.35	0.85, 0.35
horizontal width parameters A, B	4.0, 0.0	4.0, 0.0
total data	1939	3619
total unique data	902	1691
obsd data	839	1399
significance test	$F_o > 3\sigma(F_o)$	$F_o > 3\sigma(F_o)$
Refinement		
no. of parameters	55	55
weighting coefficient, g	0.001	0.0006
final R	0.0357	0.0378
$R' = [\Sigma w\Delta F^2/\Sigma wF_o^2]^{1/2}$	0.0457	0.0318

linear-chain nature by X-ray diffraction techniques and establishing the orientation of the nitro group with respect to the chain axis and the geometry at each platinum atom, and (b) the study of the electronic, infrared, Raman, and RR spectra of the complexes in order to learn more about the nature of intervalence transitions in linear-chain complexes. Preliminary results on some features of the RR spectrum of the bromide have already been reported.[11]

Experimental Section

Preparation of Complexes. The complexes $Cs_2[Pt(NO_2)(NH_3)X_2][Pt(NO_2)(NH_3)X_4]$, X = Br or I, were prepared by the methods of Muraveiskaya et al.[8,9] by the action of hydrohalic acid on *cis*-$Pt(NH_3)_2(NO_2)_2$, followed by the addition of the appropriate cesium halide. The bromide was obtained as long metallic-looking gold-green curved blades and the iodide as gold-black plates. The crystals were washed with water and alcohol and dried in air. Anal. Calcd for the bromide: N, 4.43; H, 0.48; Br, 38.00. Found: N, 4.43; H, 0.64; Br, 38.5. Anal. Calcd for the iodide: N, 3.62; H, 0.39; I, 49.33. Found: N, 3.60; H, 0.42; I, 48.6.

Crystallographic Studies. While the crystals of the iodide were well-formed, extremely thin, elongated plates, those of the bromide mostly occurred as irregular curved blades, occasionally with planar "flanges". The bromide specimen used for the X-ray data collection was a flat sliver, cut from a larger specimen, in which the plate faces and two faces forming one side of the crystal could be indexed without difficulty. The remaining cut side of the crystal was defined in terms of two faces which had directions close to crystallographic planes.

With both specimens mounted in air on glass fibers, the cell dimensions were determined by least-squares refinement of the setting angles for 25 automatically centered reflections. The cell dimensions are similar to those reported by Seth et al.[10] Both crystals gave sharp reflections, which surprised us, especially in view of the way in which the bromide sample was obtained. Intensity data were recorded on a Nonius CAD4 using Mo Kα radiation and an $\omega/2\theta$ scan in a manner described in detail previously.[12] Crystal stability (chemical and mechanical) was regularly monitored, but neither decomposition nor movement was detected. All data were corrected for *Lp* effects and for absorption. Crystal data and details of the data collection[12] are listed in Table I.

Table II

Atom Coordinates (×10^4)

	x	y	z
Pt	1882	2103	2500
Cs	4679 (1)	2229 (1)	7500
Br(1)	3270 (1)	3183 (2)	2500
Br(2)	520 (1)	964 (1)	2500
Br(3)	1980 (1)	1999 (2)	6770 (3)
N(1)	2453 (7)	261 (11)	2500
N(2)	1267 (6)	3899 (10)	2500
O(2)	1053 (6)	4391 (7)	4295 (13)

Anisotropic Temperature Factors[a] (Å^2 × 10^3)

	U_{11}	U_{22}	U_{33}	U_{23}	U_{13}	U_{12}
Pt	24	18	16	0	0	−2
Cs	40 (1)	33 (1)	33 (1)	0	0	−5
Br(1)	30 (1)	37 (1)	37 (1)	0	0	−8 (1)
Br(2)	29 (1)	29 (1)	37 (1)	0	0	−7 (1)
Br(3)	44 (1)	31 (1)	17 (1)	1 (1)	1 (1)	1 (1)
N(1)	31 (3)	29 (3)	40 (3)	0	0	−2 (3)
N(2)	15 (3)	26 (3)	23 (3)	0	0	−7 (3)
O(2)	98 (3)	58 (3)	50 (3)	−3 (3)	2 (3)	30 (3)

[a] The temperature factor exponent takes the form $-2\pi^2(U_{11}h^2a^{*2} + \ldots + 2U_{12}hka^*b^*)$.

The structure refinement of the bromide was tackled first. Our cell determination and preliminary space group identification agreed in principle with the data of Koz'min et al.,[9] and a Patterson function was interpreted to give the same heavy-atom positions. In this model, the Pt, Cs, and two Br atoms lie in a plane corresponding to $z = {}^1/_4$ for space group *Pnam*. The third bromine atom lies to one side of this plane (corresponding to space group $Pna2_1$) or, at half-occupancy, on each side (for space group *Pnam*). Attempts to refine in $Pna2_1$ produced a reasonable R value (~0.05) and only a weak ghost peak ($\rho \approx 4$ e/Å^3) across the ϕ-mirror plane in a difference map, but the thermal parameters of the lighter atoms, the nitrogen of which had moved significantly away from the origin-defining plane, were physically unreal. Continuation with the symmetry of *Pnam* and half-bromine atoms in the axial sites gave a very smooth refinement, converging at $R = 0.036$. With use of these results, the structure of the (isomorphous) iodide was then quickly refined to a final R value of 0.038. Details of the refinement for both structures are included in Table I. All calculations were performed with use of the SHELX program[13] on an ICL 2980 computer. Scattering factor data were obtained from the usual source.[14] In the refinement, the weighting scheme $\omega = 1/[\theta^2(F) + g|F_o|^2]$ was used, the g values in Table I giving acceptable agreement analyses. Final atomic positional and thermal parameters are given in Tables II and III for the bromide and iodide, respectively. Tables of observed and calculated structure factors are available as supplementary material.

Spectroscopic Studies. Electronic spectra of the complexes were recorded at room temperature on a Cary 14 spectrometer, the bromide as a pressed disk in KBr and the iodide as a Nujol mull.

Infrared spectra were recorded from pressed disks of the complexes dispersed in cesium halide (4000–200 cm^{-1}) on a Perkin-Elmer 225 spectrometer and from polythene disks (400–50 cm^{-1}) on a Beckmann IR 720M spectrometer (courtesy of Mr. A. J. Hempleman.)

Raman spectra were recorded with a Spex 1401 double monochromator with 1200-line mm^{-1} Bausch and Lomb gratings and a Spex 14018 (R6) double/triple monochromator with 1800-line mm^{-1} Jobin-Yvon holographic gratings. Radiation was provided by Coherent Radiation Models 52 Ar^+, 52 Kr^+, and 15 Ar^+ lasers. Detection was

(11) Clark, R. J. H.; Kurmoo, M. *J. Chem. Soc., Chem. Commun.* **1980**, 1258.
(12) Hursthouse, M. B.; Jones, R. A.; Malik, K. M. A.; Wilkinson, G. *J. Am. Chem. Soc.* **1979**, *101*, 4128.
(13) Sheldrick, G. M. SHELX 76 crystallographic calculation program, University of Cambridge, 1976.
(14) "International Tables of X-ray Crystallography"; Kynoch Press: Birmingham, England, 1974; Vol. IV.

Table III

Atom Coordinates ($\times 10^4$)

	x	y	z
Pt	1902	2166	2500
Cs	4700 (1)	2030 (1)	7500
I(1)	3320 (1)	3245 (1)	2500
I(2)	524	967 (1)	2500
I(3)	1993 (1)	2102 (1)	6963 (2)
N(1)	2450 (7)	411 (8)	2500
N(2)	1327 (6)	3865 (8)	2500
O(2)	1127 (7)	4380 (7)	4186 (14)

Anisotropic Temperature Factors[a] ($Å^2 \times 10^3$)

	U_{11}	U_{22}	U_{33}	U_{23}	U_{13}	U_{12}
Pt	24	20	19	0	0	−1
Cs	53 (1)	42	38	0	0	−11
I(1)	34	39	40	0	0	−10
I(2)	24	37	42	0	0	−6
I(3)	53 (1)	32	19 (1)	0	−1	−1
N(1)	48 (6)	27 (4)	26 (5)	0	0	8 (4)
N(2)	37 (5)	26 (4)	29 (5)	0	0	−2 (4)
O(2)	165 (10)	77 (5)	46 (5)	−7 (4)	9 (6)	79 (6)

[a] The temperature factor exponent takes the form $-2\pi^2(U_{11}h^2a^{*2} + \ldots + 2U_{12}hka^*b^*)$.

Table IV

Bromide		Iodide	
	Bond Lengths (Å)		
Br(1)-Pt	2.448 (3)	I(1)-Pt	2.632 (4)
Br(2)-Pt	2.439 (3)	I(2)-Pt	2.630 (4)
Br(3)-Pt	2.492 (4)	I(3)-Pt	2.711 (4)
N(1)-Pt	2.076 (13)	N(1)-Pt	2.066 (11)
N(2)-Pt	2.064 (12)	N(2)-Pt	2.033 (11)
O(2)-N(2)	1.206 (10)	O(2)-N(2)	1.205 (9)
Br(3)′-Pt	3.341 (4)	I(3)′-Pt	3.362 (4)
	Bond Angles (Deg)		
Br(2)-Pt-Br(1)	178.3	I(2)-Pt-I(1)	176.9
Br(3)-Pt-Br(1)	87.9	I(3)-Pt-I(1)	87.7
Br(3)-Pt-Br(2)	92.0	I(3)-Pt-I(2)	92.1
N(1)-Pt-Br(1)	90.9 (4)	N(1)-Pt-I(1)	89.2 (4)
N(1)-Pt-Br(2)	87.4 (4)	N(1)-Pt-I(2)	87.6 (4)
N(1)-Pt-Br(3)	86.3	N(1)-Pt-I(3)	87.3
N(2)-Pt-Br(1)	91.4 (4)	N(2)-Pt-I(1)	92.7 (4)
N(2)-Pt-Br(2)	90.3 (4)	N(2)-Pt-I(2)	90.5 (4)
N(2)-Pt-Br(3)	93.8	N(2)-Pt-I(3)	92.8
N(2)-Pt-N(1)	177.7 (4)	N(2)-Pt-N(1)	178.1 (4)
O(2)-N(2)-Pt	119.8 (6)	O(2)-N(2)-Pt	121.9 (6)
O(2)-N(2)-O(2)	120.1 (14)	O(2)-N(2)-O(2)	116.1 (13)

by photon-counting techniques employing cooled RCA C31034 photomultiplier tubes. Room temperature spectra were obtained by the spinning-sample[15] technique. Spectra at liquid-nitrogen temperature were obtained from pressed disks of the complexes dispersed in alkali halide or K_2SO_4, in conjunction with a cylindrical lens which spread the beam into a line to prevent local heating and consequent decomposition.

Four distinct single-crystal spectra were obtained by aligning the crystal ($z \equiv c$) axis first parallel and then perpendicular to the direction of polarization of the incident beam.

All band intensities (full height × full width at half-maximum) were measured relative to that of the a_1 fundamental of K_2SO_4 and corrected for the spectral response of the instruments. Band wavenumbers were calibrated by reference to the emission lines of neon.

Results and Discussion

Crystal Structures. Interatomic distances and angles are given in Table IV. The crystal structure as found corresponds to a disordered composite of octahedral $XPt^{IV}X_2(NH_3)(NO_2)X$ (X = Br or I) and square-planar $Pt^{II}X_2(NH_3)(NO_2)$ units, with the crystallographically unique Pt site comprising $^1/_2(Pt^{IV} + Pt^{II})$. We envisage that any individual chain is ordered in terms of Pt^{IV} and Pt^{II} units but that, throughout the crystal, the chains are arbitrarily slipped by $c/2$. Close examination of long-exposure photographs showed no sign of extra reflections which might double the c-axis parameter. This result parallels that obtained by Larsen and Toftlund[16] for *trans*-dichlorobis[(−)-1(*R*),2(*R*)-cyclohexanediamine]-platinum(IV)-bis[(−)-1(*R*),2(*R*)-cyclohexanediamine]platinum(II) tetrachloride, and indeed the type of structure found seems to be very general for this kind of complex.[17]

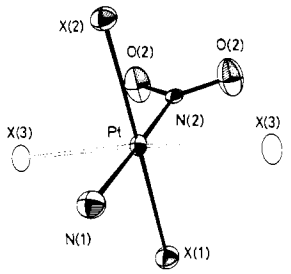

Figure 1. Crystallographic coordination geometry at the platinum atom, together with the numbering scheme adopted. The axial X(3) atoms have only half-occupancy.

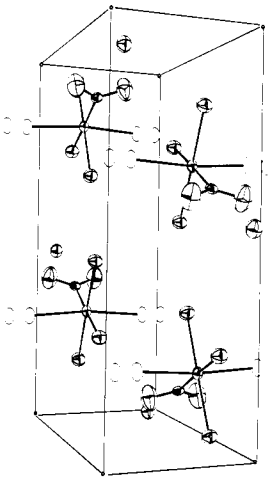

Figure 2. Perspective drawing of the contents of the unit cell.

The coordination geometry at the platinum atom in each case is illustrated in Figure 1, and the contents of the unit cell in Figure 2. Trans halogen atoms bridge the Pt^{II} and Pt^{IV} moieties in each case. In the equatorial plane, the halogen atoms are again trans to one another and in consequence the NH_3 and NO_2 groups are also trans to one another. As is typical of all halogen-bridged systems, $(Pt-X)_{br} > (Pt-X)_{ter}$, the difference being 0.05 Å in the case of the bromine and 0.08 Å in that of the iodide. The $---X-Pt^{IV}-X---Pt^{II}---$ chain deviates slightly from linearity, $\angle Pt^{IV}-Br---Pt^{II}$ being 172.3° and $\angle Pt^{IV}-I---Pt^{II}$ being 173.4°.

The nitro group is oriented in each case in the chain direction, i.e., with the NO_2 plane perpendicular to the $PtN_2(X_{eq})_2$ plane. In this orientation the NO_2 π^* orbitals are oriented for optimum overlap with the d_{xy} orbital on each platinum atom (z being the chain direction). Repulsion between the oxygen atoms and the chain halogen atoms may be responsible for slight deviation of the chain from linearity (vide supra). For both complexes, though more significantly for the iodide, the Pt–NO_2 distance is less than the Pt–NH_3 distance (by 0.012 Å in the case of the bromide, by 0.034 Å in that

(15) Kiefer, W. *Adv. Infrared Raman Spectrosc.* **1977**, *3*, 1.

(16) Larsen, K. P.; Toftlund, H. *Acta Chem. Scand., Ser. A* **1977**, *A31*, 182.
(17) Craven, D. M.; Hall, D. *Acta Crystallogr.* **1966**, *21*, 177.

Table V. Wavenumbers (cm^{-1}) of Bands Observed in the Infrared Spectra of the Complexes

X = Br	X = I	assignt
3200 s	3180 s	ν(N-H)
1615 m	1615 m	$\delta_{as}(NH_3)$
1550 m		
1425 s	1395 s	$\nu_{as}(NO_2)$
1360 s	1360 s	$\delta_{as}(NH_3)$
1325 s	1315 s	$\nu_s(NO_2)$
1300 s	1295 s	
1205 w	1195 w	$\delta_s(NH_3)$
1180 w	1175 w	
834 s	833 s	$\delta_s(NO_2)$
831 sh	828 s	
812 sh	800 w	
774 m	770 m	$\delta_r(NH_3)$
607 s	604 s	$\rho_{wag}(NO_2)$
595 s	592 s	ν(Pt-N)
307 s	302 s	$\rho_r(NO_2)$
293 s	287 s	
250 s	200 s	ν(Pt-X)
231 s	180 s	
222 s	166 s	
206 w	145 m br	
175 m		
138 m	106 w	skeletal
116 m	74 m	
73 m	66 m	

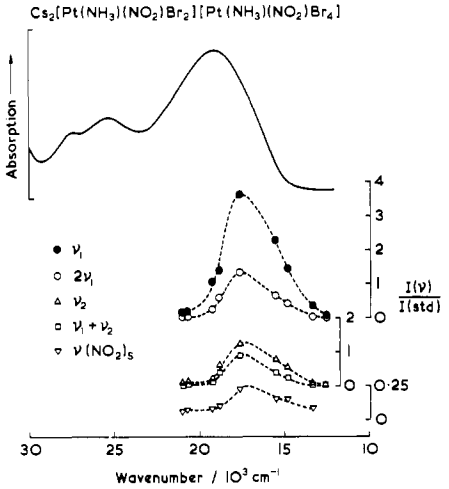

Figure 3. Electronic transmission spectrum of $Cs_2[Pt^{II}(NO_2)(NH_3)Br_2][Pt^{IV}(NO_2)(NH_3)Br_4]$ as a KBr disk at 295 K, together with the excitation profiles for the Stokes ν_1 (●), $2\nu_1$ (○), ν_2 (△), $\nu_1 + \nu_2$ (□), and $\nu_s(NO_2)$ (▽) bands at 80 K.

of the iodide). This is consistent with the belief that the nitro group is a π-acceptor ligand and that $Pt(d_\pi) \rightarrow NO_2(\pi^*)$ back-bonding will increase the strength of, and thus shorten, the Pt–NO_2 bonds relative to the Pt–NH_3 bonds. Moreover, the fact that Pt–NO_2 distance is less for the iodide than for the bromide (by 0.031 Å) is consistent with the argument that the effective nuclear charge on the platinum atoms is lower for the iodide than for the bromide (on account of the lower electronegativity of iodine than bromine), and hence that the $Pt(d_\pi) \rightarrow NO_2(\pi^*)$ back-bonding would be the greater for the iodide; this conclusion is substantiated by the lower symmetric and asymmetric $\nu(NO_2)$ band wavenumbers for the iodide than for the bromide (Table V).

Electronic Spectra. Both complexes are dichroic and have a metallic sheen: gold-green (bromide) and gold-black (iodide). However, on being ground into a powder, the bromide turns red and the iodide black. The electronic transmission spectra, which are effectively the sums of $\epsilon_\parallel$ and $\epsilon_\perp$ in each case, show broad bands in the visible and near-infrared regions. The bromide (KBr disk) shows three maxima at 27 500, 25 300, and 19 000 cm^{-1}, the last being the most intense (Figure 3), and the iodide (Nujol mull) shows two maxima at 16 700 and 12 800 cm^{-1} (Figure 4). The lowest energy bands in each case, which are polarized along the chain axis, are assigned to the $Pt^{II} \rightarrow Pt^{IV}$ intervalence transition by analogy with previous results for other chain complexes.[1-7] The bands at higher energies are probably $X \rightarrow Pt$ charge-transfer bands, although analogous bands are not observed in the electronic spectra of the complexes $[Pt(LL)_2][Pt(LL)_2X_2]Y_4$ and $[Pt(en)X_2][Pt(en)X_4]$, where LL = en, pn, or tn[3,4], X = Cl, Br, or I, and Y = ClO_4 or BF_4 (en = 1,2-diaminoethane, pn = 1,2-diaminopropane, and tn = 1,3-diaminopropane).

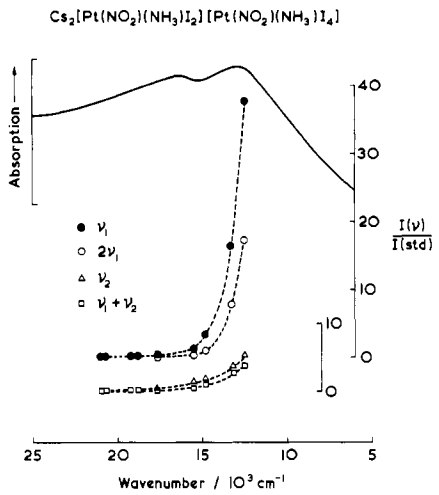

Figure 4. Electronic transmission spectrum of $Cs_2[Pt^{II}(NO_2)(NH_3)I_2][Pt^{IV}(NO_2)(NH_3)I_4]$ as a Nujol mull at 295 K, together with the excitation profiles for the Stokes ν_1 (●), $2\nu_1$ (○), ν_2 (△), and $\nu_1 + \nu_2$ (□) bands at 80 K.

Infrared Spectra. The wavenumbers and assignments of the bands observed in the infrared spectra of the complexes are listed in Table V. The bands at 1325 (bromide) and 1315 (iodide) and at 607 (bromide) and 604 cm^{-1} (iodide) are clear indications that the complexes are nitro- rather than nitrito ones, the latter being characterized by bands between 1485–1400 and 1110–1050 cm^{-1} due to the ν(N=O) and ν(N—O) modes, respectively.[18] The band at 595 (bromide) and 592 cm^{-1} (iodide) are assigned to ν_{as}(PtN) asymmetric stretching fundamentals, while those at 250, 231, and 222 cm^{-1} (bromide) and at 200, 180, and 166 cm^{-1} (iodide) are assigned to ν_{as}(PtBr) and ν_{as}(PtI) asymmetric stretching fundamentals, respectively.

Resonance Raman Spectra. The Raman spectra of the two complexes display a striking dependence on both exciting frequency as well as on sample temperature. A room-temperature Raman spectrum of the bromide with blue or red lines consists of bands attributable only to fundamentals, but with yellow or green lines; overtones of both ν_1 and ν_2, the symmetric $X-Pt^{IV}-X$ stretching modes (axial and equatorial, respectively) are readily apparent, together with combination bands involving each mode. The Raman spectrum of the iodide at room temperature consists only of bands attributable to fundamentals with all lines except for the deep red Kr^+ ones at 752.5 and 799.3 nm. Much better resolved spectra result if the samples are cooled to ca. 80 K.

Irradiation within the contour of the $Pt^{II} \rightarrow Pt^{IV}$ intervalence band centered at 19 000 cm^{-1} for the (powdered) bromide and 12 800 cm^{-1} for the (powdered) iodide leads to the development of very intense and detailed RR spectra. In the case of the bromide (Figure 5), 11 progressions of three or more members

(18) Nakamoto, K. "Infrared and Raman Spectra of Inorganic and Coordination Compounds"; Wiley-Interscience: New York, 1978.

Table VI. Wavenumbers (cm^{-1}), Relative Intensities, Fwhm, and Assignments of Bands Observed in the RR Spectrum of $Cs_2[Pt(NO_2)(NH_3)Br_2][Pt(NO_2)(NH_3)Br_4]$ at ca. 80 K

$\tilde{\nu}/cm^{-1}$ [a]	$I(\nu)/I(\nu_1)$	$\Delta\tilde{\nu}_{1/2}/cm^{-1}$	assignts
72.3			
88.0			
105.9			
117.2			
138.5			
177.3	1.0	4.3	ν_1
206.9	0.37	5.9	ν_2
232.0			
250.0			$\nu_1 + 72.3$
282.1			$\nu_1 + 105.9$
315.9			$\nu_1 + 138.5$
355.8	0.48	7.5	$2\nu_1$
385.0	0.30	7.5	$\nu_1 + \nu_2$
413.3	0.12	9.5	$2\nu_2$
459.7			$2\nu_1 + 105.9$
492.5			$2\nu_1 + 138.5$
532.4	0.28	11.8	$3\nu_1$
562.8	0.23	10.2	$2\nu_1 + \nu_2$
591.4	0.11	11.0	$\nu_1 + 2\nu_2$
619.2	0.04	13.4	$3\nu_2$
637.4			$3\nu_1 + 105.9$
669.5			$3\nu_1 + 138.5$
708.3	0.14	15	$4\nu_1$
739.7	0.14	13.4	$3\nu_1 + \nu_2$
769.0	0.09	13.4	$2\nu_1 + 2\nu_2$
797.7	0.03	15	$\nu_1 + 3\nu_2$
832.9	0.02	3.1	$\delta_s(NO_2)$
883.9	0.08	20	$5\nu_1$
916.1	0.12	18	$4\nu_1 + \nu_2$
946.4	0.06	16	$3\nu_1 + 2\nu_2$
975.6	0.03	16	$2\nu_1 + 3\nu_2$
1010.2			$\nu_1 + \delta_s(NO_2)$
1040.6			$\nu_2 + \delta_s(NO_2)$
1058.7	0.03	22	$6\nu_1$
1090.8	0.05	20	$5\nu_1 + \nu_2$
1122.8	0.03	17	$4\nu_1 + 2\nu_2$
1154	0.02	19	$3\nu_1 + 3\nu_2$
1187			$2\nu_1 + \delta_s(NO_2)$
1217			$\nu_1 + \nu_2 + \delta_s(NO_2)$
1231			$7\nu_1$
1265	0.02	>22	$6\nu_1 + \nu_2$
1298			$5\nu_1 + 2\nu_2$
1334	0.04	3.9	$\nu_s(NO_2)$
1363			$3\nu_1 + \delta_s(NO_2)$
1394			$2\nu_1 + \nu_2 + \delta_s(NO_2)$
1435			$7\nu_1 + \nu_2$
1475			$6\nu_1 + 2\nu_2$
1512			$\nu_1 + \nu_s(NO_2)$
1542			$\nu_2 + \nu_s(NO_2)$
1689			$2\nu_1 + \nu_s(NO_2)$
1720			$\nu_1 + \nu_2 + \nu_s(NO_2)$
1746			$2\nu_2 + \nu_s(NO_2)$
1867			$3\nu_1 + \nu_s(NO_2)$

[a] Obtained as a KBr disk with 568.2-nm (Kr^+) excitation.

were observed, in nine of which, ν_1, $\nu_s(Br-Pt^{IV}-Br)$ at ca. 178 cm^{-1}, acts as the progression-forming mode. The latter is confirmed to be totally symmetric on the basis of single-crystal polarization studies (vide infra). The progresssions in ν_1 other than the main $\nu_1\nu_1$ one are based on one or more quanta of another Raman-active fundamental, viz., ν_2 (at 207 cm^{-1}), $2\nu_2$, $3\nu_2$, $\delta(NO_2)_s$ (at 833 cm^{-1}), $\nu(NO_2)_s$ (at 1334 cm^{-1}), and other unidentified modes. There are also three shorter progressions in which ν_2 acts as the progression-forming mode. The wavenumbers, fwhm, and intensities (relative to ν_1) of the bands observed in the RR spectrum are listed in Table VI.

The RR spectrum of the iodide (Figure 6) is also very intense and detailed with either 752.5- or 799.3-nm excitation, but the amount of detail is rather less than for the bromide; this is possibly because for the optimum RR spectrum one would need an excitation wavelength beyond 800 nm. The results for this complex are given in Table VII.

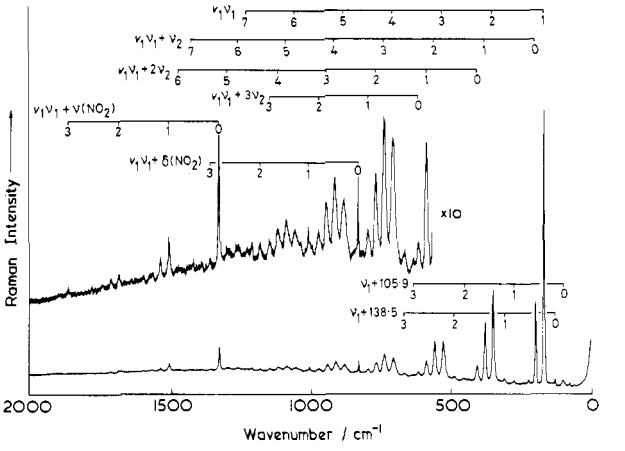

Figure 5. Resonance Raman spectrum of $Cs_2[Pt^{II}(NO_2)(NH_3)Br_2][Pt^{IV}(NO_2)(NH_3)Br_4]$ at ca. 80 K (λ_0 = 568.2 nm, slit width ~1 cm^{-1}).

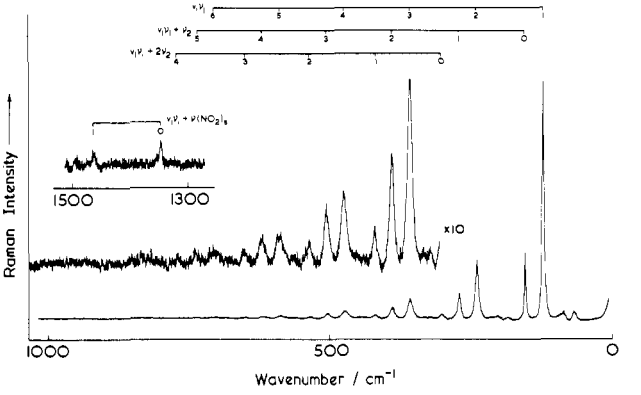

Figure 6. Resonance Raman spectrum of $Cs_2[Pt^{II}(NO_2)(NH_3)I_2][Pt^{IV}(NO_2)(NH_3)I_4]$ at ca. 80 K (λ_0 = 752.5 nm, slit width ~1.5 cm^{-1}).

Table VII. Wavenumbers (cm^{-1}), Relative Intensities, Fwhm, and Assignments of Bands Observed in the RR Spectrum of $Cs_2[Pt(NO_2)(NH_3)I_2][Pt(NO_2)(NH_3)I_4]$ at 80 K

$\tilde{\nu}/cm^{-1}$ [a]	$I(\nu)/I(\nu_1)$	$\Delta\tilde{\nu}_{1/2}/cm^{-1}$	assignts
60.2			
82.8			
117.8	1.00	4.3	ν_1
149.0	0.24	3.7	ν_2
179.0			$\nu_1 + 60.2$
198.0			$\nu_1 + 82.8$
235.8	0.42	7.1	$2\nu_1$
266.1	0.17	6.9	$\nu_1 + \nu_2$
296.5	0.05	9.1	$2\nu_2$
315.7			$2\nu_1 + 82.8$
353.0	0.23	10.6	$3\nu_1$
383.8	0.10	8.7	$2\nu_1 + \nu_2$
414.4	0.05	11.0	$\nu_1 + 2\nu_2$
469.7	0.09	12.6	$4\nu_1$
500.9	0.07	11.8	$3\nu_1 + \nu_2$
530.7	0.03	12.6	$2\nu_1 + 2\nu_2$
585.4	0.06	15	$5\nu_1$
616.8	0.06	16	$4\nu_1 + \nu_2$
649.3	~0.01		$3\nu_1 + 2\nu_2$
705	0.04	~20	$6\nu_1$
735	0.03	~20	$5\nu_1 + \nu_2$
770	<0.01		$4\nu_1 + 2\nu_2$
1321	<0.01		$\nu_s(NO_2)$
1438	<0.01		$\nu_1 + \nu_s(NO_2)$

[a] Obtained as a CsI disk with 752.5 nm (Kr^+) excitation.

Table VIII. Summary of Progressions Observed in the Resonance Raman Spectra of the Complexes $Cs_2[Pt(NO_2)(NH_3)X_2][Pt(NO_2)(NH_3)X_4]$

X = Br		X = I	
$\upsilon_1\nu_1$	$\upsilon_1 = 1$–7	$\upsilon_1\nu_1$	$\upsilon_1 = 1$–6
$\upsilon_1\nu_1 + \nu_2$	$\upsilon_1 = 0$–7	$\upsilon_1\nu_1 + \nu_2$	$\upsilon_1 = 0$–5
$\upsilon_1\nu_1 + 2\nu_2$	$\upsilon_1 = 0$–6	$\upsilon_1\nu_1 + 2\nu_2$	$\upsilon_1 = 0$–4
$\upsilon_1\nu_1 + 3\nu_2$	$\upsilon_1 = 0$–3		
$\upsilon_1\nu_1 + \delta_s(NO_2)$	$\upsilon_1 = 0$–3		
$\upsilon_1\nu_1 + \nu_s(NO_2)$	$\upsilon_1 = 0$–3	$\upsilon_1\nu_1 + \nu_s(NO_2)$	$\upsilon_1 = 0, 1$
$\upsilon_1\nu_1 + \nu_2 + \delta_s(NO_2)$	$\upsilon_1 = 0$–2		
$\upsilon_1\nu_1 + \nu_2 + \nu_s(NO_2)$	$\upsilon_1 = 0, 1$		
$\upsilon_1\nu_1 + 72.3$	$\upsilon_1 = 0, 1$	$\upsilon_1\nu_1 + 60.2$	$\upsilon_1 = 0, 1$
$\upsilon_1\nu_1 + 105.9$	$\upsilon_1 = 0$–3	$\upsilon_1\nu_1 + 82.8$	$\upsilon_1 = 0$–2
$\upsilon_1\nu_1 + 138.5$	$\upsilon_1 = 0$–3		
$\upsilon_2\nu_2$	$\upsilon_2 = 1$–3	$\upsilon_2\nu_2$	$\upsilon_2 = 1, 2$
$\upsilon_2\nu_2 + \delta_s(NO_2)$	$\upsilon_2 = 0, 1$		
$\upsilon_2\nu_2 + \nu_s(NO_2)$	$\upsilon_2 = 0$–2		

Table IX. Summary of Data on Complexes Studied

	$Cs_2[Pt(NO_2)(NH_3)X_2][Pt(NO_2)(NH_3)X_4]$	
	X = Br	X = I
crystal[a]	green-gold needles	gold-black plates
powder	red	black
mixed-valence[b] band max/cm^{-1}	19 000	12 800
excitation-profile band max/cm^{-1}	17 600	<12 500
ω_1/cm^{-1}	179.0 ± 0.3	118.3 ± 0.3
ω_2/cm^{-1}	207.4 ± 0.3	150 ± 1
x_{11}/cm^{-1}	−0.39 ± 0.04	−0.16 ± 0.04
x_{12}/cm^{-1}	0.0 ± 0.1[c]	−0.4 ± 0.2
x_{22}/cm^{-1}	−0.25 ± 0.05	−0.7 ± 0.5
main progressions (at ca. 80 K)	$7\nu_1$, $3\nu_2$	$6\nu_1$, $2\nu_2$
$I(2\nu_1)/I(\nu_1)$[d]	0.48	0.42
$I(\nu_2)/I(\nu_1)$[d]	0.37	0.24
$\underline{d}(Pt^{II}$–$Pt^{IV})$/Å	5.820	6.063

[a] By reflected light. [b] By transmission. [c] From the wavenumbers of the members of the $\upsilon_1\nu_1 + \delta_s(NO_2)$ progression in the spectrum of the bromide, the cross-term $x_{1\delta}$ was determined to be −0.8 ± 0.2 cm^{-1}. [d] At resonance.

A summary of the assignments of the observed RR progressions for both complexes is given in Table VIII, from which it is clear that ν_1 plays the dominant role in each spectrum. Thus the principal geometric change undergone by each molecule on excitation to the intervalence state is an elongation of the axial Pt^{IV}–X bonds. This feature is typical of linear-chain complexes. However, it is clear that other modes (e.g., ν_2) are affected on excitation to the intervalence state, and this to an extent which appears to be greater than for other (cationic or neutral) chain complexes.[1] Particularly interesting is the involvement of the symmetric stretching and bending modes of the nitro group. This suggests very reasonably that the $Pt^{II} \rightarrow Pt^{IV}$ intervalence transition alters the effective nuclear charge on each platinum atom and thus affects the $Pt(d_{xy}) \rightarrow NO_2(\pi^*)$ back-bonding and hence the equilibrium geometry of the NO_2 group in the intervalence state.

The observation of many combination-band progressions of the sort $\upsilon_1\nu_1 + \upsilon_2\nu_2$ implies that the intervalence-state potential surface is displaced, with respect to the ground state, along more than one normal coordinate, but it is unclear whether or not this is a consequence of the Duschinsky effect.[19-21]

Analysis of the extensive RR data on these complexes by standard procedures[22] allows the calculation of (approximate) values for the harmonic wavenumbers, ω_1 and ω_2, and of the anharmonicity constants x_{11}, x_{12}, and (in the case of the bromide) $x_{1\delta}$. These results are included in Table IX. Both of the progression-forming modes are only very slightly anharmonic, x_{jj}/ω_j being in the range 0.1%–0.4%.

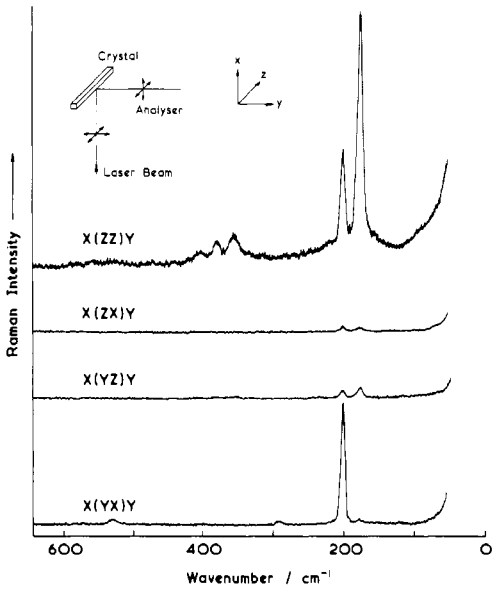

Figure 7. Resonance Raman spectrum of a single crystal of $Cs_2[Pt^{II}(NO_2)(NH_3)Br_2][Pt^{IV}(NO_2)(NH_3)Br_4]$ at room temperature (λ_0 = 568.2 nm, slit width ~4 cm^{-1}). The crystallographic and needle z axis is coincident with the space-fixed z axis, and the $Pt–Br_{eq}$ bond direction is coincident with the space-fixed x axis for all the spectra shown.

The RR spectrum of an oriented single crystal (~2 × 0.3 × 0.3 mm) of the bromide at room temperature is shown in Figure 7. The most intense and detailed spectrum is obtained when the electric vector of the incident beam is parallel to the chain direction (z) and also to the analyser, i.e., $x(zz)y$ in Porto's nomenclature. Thus, it is clear that most bands in the RR spectrum are polarized and therefore attributable to totally symmetric modes. In the $x(yx)y$ orientation, a strong ν_2 band appears (indicating that it is polarized perpendicular to ν_1) together with weak bands at 290 and 530 cm^{-1} which are probably attributable to $\rho_r(NO_2)$ and $\nu_s(Pt–NH_3)$ fundamentals, respectively.[18] The observation of a weak ν_2 band in the $x(zz)y$ spectrum is doubtless a consequence of the fact that the $Pt–X_{ax}$ direction is not exactly perpendicular to the $PtN_2(X_{eq})_2$ plane in the crystal.

The excitation profiles of the ν_1, $2\nu_1$, ν_2, $\nu_1 + \nu_2$, and $\nu_s(NO_2)$ bands for the bromide are included in Figure 3. They all maximize at 17 600 cm^{-1}, i.e., about 1400 cm^{-1} on the low-energy side of the intervalence-band maximum; this behavior is typical of linear chain complexes.[1] The excitation profiles of the ν_1, $2\nu_1$, ν_2, and $\nu_1 + \nu_2$ bands of the iodide are included in Figure 4. The bands are clearly all enhanced within the contour of the intervalence band, their maximum intensities again being on the low-energy side of the intervalence band; however, owing to the lack of available lines of wavelength greater than 800 nm, we could not establish the wavelengths of the maximum intensities. These results clearly demonstrate that ν_1 is the most enhanced band at resonance, but that other nonaxial modes are also coupled to the intervalence band.

Conclusion

Table IX consists of a summary of the key properties of the two complexes studied. Their one-dimensionality is evident from their electrical conductance,[10] gross optical dichroism, metallic luster, and RR spectra, as well as from the X-ray crystal structure analyses. The bond lengths and angles are typical of those in square-planar and octahedrally coordinated

(19) Duschinsky, F. *Acta Physicochim. URSS* **1937**, *7*, 551.
(20) Craig, D. P.; Small, G. J. *J. Chem. Phys.* **1969**, *50*, 3827.
(21) Siebrand, W.; Zgierski, M. Z. *Chem. Phys. Lett.* **1979**, *62*, 3.
(22) Campbell, J. R.; Clark, R. J. H. *Mol. Phys.* **1978**, *36*, 1133.

platinum complexes, and the Pt–NO_2 bond lengths imply that there is significant $Pt(d_{xy}) \rightarrow NO_2(\pi^*)$ back-bonding in the complexes. This result is also implicit in the RR results, in that the long observed progressions in the $X-Pt^{IV}-X$ axial symmetric stretching mode on irradiation into the intervalence band are accompanied by other weaker progressions involving not only the $X-Pt^{IV}-X$ equatorial symmetric stretching mode but also the symmetric NO_2 stretching and bending modes. The $Pt^{II} \rightarrow Pt^{IV}$ intervalence band, although axial, clearly has far reaching, though small, consequential effects on the equatorial bonds, presumably on account of both the π-acceptor nature of the nitro group as well as the anionic nature of the linear-chain, factors which apparently also give rise[10] to the observed low $4f_{7/2}$ and $4f_{9/2}$ Pt binding energies in the complexes.

Acknowledgment. We thank the Science Research Council and the University of London for financial support and Johnson-Matthey Ltd. for the loan of chemicals.

Registry No. $Cs_2[Pt^{II}(NO_2)(NH_3)Br_2][Pt^{IV}(NO_2)(NH_3)Br_4]$, 79056-31-8; $Cs_2[Pt^{II}(NO_2)(NH_3)I_2][Pt^{IV}(NO_2)(NH_3)I_4]$, 79056-34-1.

Supplementary Material Available: Listings of observed and calculated structure amplitudes for the two compounds (10 pages). Ordering information is given on any current masthead page.

Contribution from the Department of Chemistry, The University of Calgary, Calgary, Alberta, Canada, T2N 1N4, and l'Institut de Chimie Minérale et Analytique, Université de Lausanne, CH-1005, Lausanne, Switzerland

High-Pressure Oxygen-17 Fourier Transform Nuclear Magnetic Resonance Spectroscopy. Mechanism of Water Exchange on Iron(III) in Acidic Aqueous Solution

THOMAS W. SWADDLE* and ANDRÉ E. MERBACH*

Received February 2, 1981

The rate of exchange of water between iron(III) perchlorate and bulk acidic aqueous solution has been determined as a function of pressure (0.1–240 MPa) at 382.8 K by oxygen-17 NMR line-broadening measurements. The pseudo-first-order rate coefficient k is given by $k = k_1^\circ \exp(-P\Delta V_1^*/RT) + k_2^\circ[H^+]^{-1} \exp(-P\Delta V_2^*/RT)$, where k_1° (representing exchange on $Fe(H_2O)_6^{3+}$) = 6.8×10^4 s^{-1}, $\Delta V_1^* = -5.4$ cm^3 mol^{-1}, $k_2^\circ = 11.4 \times 10^4$ mol kg^{-1} s^{-1}, and $\Delta V_2^* = +7.8$ cm^3 mol^{-1} for ionic strength 6.0 mol kg^{-1} ($HClO_4/NaClO_4$). Optical measurements gave a temperature-independent volume of acid ionization for $Fe(H_2O)_6^{3+}$ of +0.8 cm^3 mol^{-1}, so that the volume of activation ΔV_{OH}^* for water exchange on $Fe(H_2O)_5OH^{2+}$ is +7.0 cm^3 mol^{-1}. These data are consistent with dissociative activation for substitution in $Fe(H_2O)_5OH^{2+}$ but associative activation in $Fe(H_2O)_6^{3+}$.

Introduction

In 1974, one of us pointed out[1] that the pattern of rates of substitution of water by other ligands in aqueous $Fe(H_2O)_5OH^{2+}$ and $Fe(H_2O)_6^{3+}$ was consistent with dissociative activation in the former case, as was then considered to be quite general for "labile" octahedral complexes, but *associative* in the latter. Subsequently, other workers have drawn similar mechanistic conclusions on the basis of kinetic studies at both high[2-4] and atmospheric[5,6] pressures. In particular, the recent NMR study by Grant and Jordan[6] has provided a key piece of evidence favoring this mechanistic assignment, viz., the rate of exchange of solvent water with $Fe(H_2O)_6^{3+}$ and with $Fe(H_2O)_5OH^{2+}$.

In this paper, we report our confirmation of the findings of Grant and Jordan[6] and an extension of their atmospheric-pressure study to high pressures (to 240 MPa) since, as we have argued elsewhere,[1,7-9] pressure effects can provide useful criteria of mechanism in solvent exchange reactions.

Experimental Section

Iron(III) perchlorate ($Fe(ClO_4)_3 \cdot nH_2O$, Fluka AG) was analyzed as received and then used without further treatment; the Mn content was shown to be not more than 3 μg/g, and the Fe content corresponded to a formula weight of 495.1 (i.e., $n \approx 8$). The solid was kept in a closed container inside a desiccator, and stock solutions were prepared by weight by dissolution of samples of the solid, weighed in closed capsules together with $NaClO_4 \cdot H_2O$ (Merck), in appropriate amounts of 69.1% $HClO_4$ (Merck) and distilled water. Solutions for ^{17}O NMR studies at high pressure were prepared by mixing weighed amounts of the stock solutions with multiply redistilled ^{17}O-enriched water (Yeda, normalized in ^1H, 25.5 atom % ^{17}O, 33.1 atom % ^{18}O) to yield a $H_2{}^{17}O$/(total water) ratio of about 1:10 and an ionic strength I of 6.0 m (m = mol kg^{-1}); the apparent molecular weight of water in these solutions was therefore 18.56. Preliminary studies at atmospheric pressure were made with similar electrolyte concentrations but an $H_2{}^{17}O$/(total water) ratio of 1:25. All surfaces with which the solutions would come in contact were first cleaned with $K_2S_2O_8$/concentrated H_2SO_4, rinsed thoroughly with distilled water, and air-dried at 110 °C; great care was taken at all stages to avoid contamination with oxidizable matter (cf. precautions advocated by Grant and Jordan[6]).

NMR measurements were made with a Bruker WP-60 spectrometer (8.13 MHz ^{17}O) in the ^{19}F lock mode. Preliminary variable-temperature studies were made at ~0.1 MPa with the solution sample sealed in vacuo in a 9-mm sphere fitting inside a 10-mm NMR tube. High-pressure studies (0.1–240 MPa, 382.8 K) were made with the use of an assembly, similar to that described elsewhere for ^{13}C studies but with the coil wound and tuned appropriately for ^{17}O resonance, in which the sample was contained in a glass tube (2.0-mm i.d.) fitted with a collapsible Teflon® outer tube closed with a Vespel® plug; thus, the sample was in contact with borosilicate glass, polytetrafluoroethylene, and polyimide resin during the NMR experiments. The temperature was controlled with circulating oil to ±0.1 K and monitored with an internal Pt resistance thermometer (referred to

* Address correspondence as follows: T.W.S., The University of Calgary; A.E.M., Université de Lausanne.

(1) Swaddle, T. W. *Coord. Chem. Rev.* **1974**, *14*, 217.
(2) Hasinoff, B. B. *Can. J. Chem.* **1976**, *54*, 1820.
(3) Jost, A. *Ber. Bunsenges. Phys. Chem.* **1976**, *80*, 316.
(4) Hasinoff, B. B. *Can. J. Chem.* **1979**, *57*, 77.
(5) Gomwalk, U. D.; Lappin, A. G.; McCann, J. P.; McAuley, A. *Inorg. Chim. Acta* **1977**, *24*, 39.
(6) Grant, M.; Jordan, R. B. *Inorg. Chem.* **1981**, *20*, 55.
(7) Newman, K. E.; Merbach, A. E. *Inorg. Chem.* **1980**, *19*, 2481.
(8) Swaddle, T. W. *Inorg. Chem.* **1980**, *19*, 3203.
(9) Swaddle, T. W. In "High Pressure Science and Technology"; Timmerhaus, K. D., Barber, M. S., Eds.; Plenum Press: New York, 1979; Vol. 1, p 631.
(10) Monnerat, A.; Moore, P.; Newman, K. E.; Merbach, A. E. *Inorg. Chim. Acta* **1981**, *47*, 139.
(11) Vanni, H.; Earl, W. L.; Merbach, A. E. *J. Magn. Reson.* **1978**, *29*, 11.
(12) Earl, W. L.; Vanni, H.; Merbach, A. E. *J. Magn. Reson.* **1978**, *30*, 571.

0020-1669/81/1320-4212$01.25/0